

# Determination of two-photon exchange amplitudes from elastic electron-proton scattering data

Julia Guttmann<sup>1</sup>, Nikolai Kivel<sup>1,2,3</sup>, Mehdi Meiziane<sup>4</sup>, and Marc Vanderhaeghen<sup>1,2</sup>

<sup>1</sup> Institut für Kernphysik, Johannes Gutenberg-Universität, D-55099 Mainz, Germany

<sup>2</sup> Helmholtz Institut Mainz, Johannes Gutenberg-Universität, D-55099 Mainz, Germany

<sup>3</sup> Petersburg Nuclear Physics Institute, Gatchina, St. Petersburg 188350, Russia

<sup>4</sup> Physics Department, College of William and Mary, Williamsburg, VA 23187, USA

Received: date / Revised version: date

**Abstract.** Using the available cross section and polarization data for elastic electron-proton scattering, we provide an extraction of the two-photon exchange amplitudes at a common value of four-momentum transfer, around  $Q^2 = 2.5 \text{ GeV}^2$ . This analysis also predicts the  $e^+p/e^-p$  elastic scattering cross section ratio, which will be measured by forthcoming experiments.

**PACS.** 25.30.Bf Elastic electron scattering – 13.40.Gp Electromagnetic form factors – 14.20.Dh Protons and neutrons

The electromagnetic form factors (FFs) of the nucleon have been explored extensively during the last 50 years with ever increasing accuracy. The tool to extract the electromagnetic FFs is provided by the one-photon ( $1\gamma$ ) exchange approximation to elastic electron-nucleon scattering. Precision measurements of the proton electric to magnetic FF ratio at larger momentum transfers using polarization experiments [1,2,3,4] have revealed significant discrepancies in recent years with unpolarized experiments using the Rosenbluth technique [5,6,7], when analyzing both within the  $1\gamma$ -exchange framework. As both techniques were scrutinized and their findings confirmed by different experimental groups and using different set-ups, it became clear that some other explanation was needed to explain the difference. It was proposed that two-photon ( $2\gamma$ ) exchange processes are the most likely explanation of this difference [8,9,10]. Their study has received a lot of attention lately, see [11] for a recent review (and references therein), and [12] for a global analysis of elastic  $ep$  scattering including a model for the  $2\gamma$  corrections.

In recent years dedicated experiments were performed to test the Rosenbluth method [7] and to measure the  $2\gamma$ -corrections to the polarization observables [13]. Using the theoretical framework to describe elastic  $ep$  scattering beyond the  $1\gamma$ -approximation, as laid out in Ref. [8], both experiments allow for the first time to provide an empirical determination of the  $2\gamma$ -amplitudes at a common value of the momentum transfer,  $Q^2 = 2.64 \text{ GeV}^2$ . We extract the resulting  $2\gamma$ -amplitudes in this work and provide predictions for forthcoming experiments.

To describe the process,  $l(k) + N(p) \rightarrow l(k') + N(p')$ , we adopt the definitions:  $P = (p + p')/2$ ,  $K = (k + k')/2$ ,

$q = k - k'$ , and choose  $Q^2 = -q^2$  and  $\nu = K \cdot P$  as the independent kinematical invariants. Neglecting the electron mass, the elastic  $ep$  scattering amplitude can be expressed through 3 independent structures [8]:

$$T_{h,\lambda'_N\lambda_N} = (e^2/Q^2) \bar{u}(k',h) \gamma_\mu u(k,h) \times \bar{u}(p',\lambda'_N) \left( \tilde{G}_M \gamma^\mu - \tilde{F}_2 \frac{P^\mu}{M} + \tilde{F}_3 \frac{\gamma \cdot KP^\mu}{M^2} \right) u(p,\lambda_N), \quad (1)$$

with  $e$  the proton charge,  $M$  its mass,  $h = \pm 1/2$  the electron helicity and  $\lambda_N$  ( $\lambda'_N$ ) the incoming (outgoing) proton helicities. In Eq. (1),  $\tilde{G}_M$ ,  $\tilde{F}_2$ ,  $\tilde{F}_3$  are complex functions of  $\nu$  and  $Q^2$ . For convenience, we also use  $\tilde{G}_E \equiv \tilde{G}_M - (1 + \tau)\tilde{F}_2$ , with  $\tau \equiv Q^2/(2M)^2$ . To separately identify the  $1\gamma$ - and  $2\gamma$ -exchange contributions, we use the decomposition  $\tilde{G}_M = G_M + \delta\tilde{G}_M$ , and  $\tilde{G}_E = G_E + \delta\tilde{G}_E$ , where  $G_M$  and  $G_E$  are the usual proton magnetic and electric FFs, which are functions of  $Q^2$  only and are defined from matrix elements of the electromagnetic current. The amplitudes  $\tilde{F}_3$ ,  $\delta\tilde{G}_M$ , and  $\delta\tilde{G}_E$ , originate from processes involving the exchange of at least two photons, and are of order  $e^2$ . When calculating observables beyond the  $1\gamma$ -approximation, it is convenient to express the real parts ( $\mathcal{R}$ ) of the  $2\gamma$ -amplitudes relative to the magnetic FF as:

$$\begin{aligned} Y_M &\equiv \mathcal{R}(\delta\tilde{G}_M/G_M), & Y_E &\equiv \mathcal{R}(\delta\tilde{G}_E/G_M), \\ Y_3 &\equiv (\nu/M^2) \mathcal{R}(\tilde{F}_3/G_M). \end{aligned} \quad (2)$$

The reduced  $e^-p \rightarrow e^-p$  cross section including the  $2\gamma$ -corrections becomes [8]

$$\frac{\sigma_R}{G_M^2} = 1 + \frac{\varepsilon}{\tau} \frac{G_E^2}{G_M^2} + 2Y_M + 2\varepsilon \frac{G_E}{\tau G_M} Y_E + 2\varepsilon \left(1 + \frac{G_E}{\tau G_M}\right) Y_3 + \mathcal{O}(\varepsilon^4), \quad (3)$$

where  $\varepsilon$  is the virtual photon polarization parameter. The corresponding expression for the elastic  $e^+p \rightarrow e^+p$  cross section is obtained by changing the sign in front of the  $2\gamma$ -amplitudes in Eq. (3).

In the  $1\gamma$ -exchange (Born) approximation, the double polarization observables are given by :

$$P_l^{\text{Born}} = \sqrt{1 - \varepsilon^2} (2h) \left(1 + \frac{\varepsilon}{\tau} \frac{G_E^2}{G_M^2}\right)^{-1}, \quad (4)$$

$$P_t^{\text{Born}} = -\sqrt{\frac{2\varepsilon(1 - \varepsilon)}{\tau}} (2h) \left(1 + \frac{\varepsilon}{\tau} \frac{G_E^2}{G_M^2}\right)^{-1} \frac{G_E}{G_M}. \quad (5)$$

Including  $2\gamma$ -corrections, the polarization transfer ratio can be written as [8]:

$$-\sqrt{\frac{\tau(1 + \varepsilon)}{2\varepsilon}} \frac{P_t}{P_l} = \frac{G_E}{G_M} + Y_E - \frac{G_E}{G_M} Y_M + \left(1 - \frac{2\varepsilon}{1 + \varepsilon} \frac{G_E}{G_M}\right) Y_3 + \mathcal{O}(\varepsilon^4). \quad (6)$$

For  $P_l$  separately, its expression relative to the  $1\gamma$ -result of Eq. (4) is given by :

$$\begin{aligned} \frac{P_l}{P_l^{\text{Born}}} &= 1 - 2\varepsilon \left(1 + \frac{\varepsilon}{\tau} \frac{G_E^2}{G_M^2}\right)^{-1} \\ &\times \left\{ \left[ \frac{\varepsilon}{1 + \varepsilon} \left(1 - \frac{G_E^2}{\tau G_M^2}\right) + \frac{G_E}{\tau G_M} \right] Y_3 \right. \\ &\left. + \frac{G_E}{\tau G_M} \left[ Y_E - \frac{G_E}{G_M} Y_M \right] \right\} + \mathcal{O}(\varepsilon^4). \quad (7) \end{aligned}$$

We can make an estimate of the  $2\gamma$ -amplitudes from the recent data for the  $\varepsilon$ -dependence of  $P_t/P_l$  and  $P_l/P_l^{\text{Born}}$  at  $Q^2 = 2.5 \text{ GeV}^2$ , as measured by the JLab/Hall C experiment [13], and combine them with the precision Rosenbluth measurements of  $\sigma_R$  performed at JLab/Hall A [7], where data exist at a similar value  $Q^2 = 2.64 \text{ GeV}^2$ . The combination of both experiments allows for the first time to have three observables at a same  $Q^2$  value to extract the  $\varepsilon$ -dependence of the three  $2\gamma$ -amplitudes  $Y_M$ ,  $Y_E$ , and  $Y_3$ , which are functions of both  $Q^2$  and  $\varepsilon$ .

We start with the data for  $P_t/P_l$  as shown on Fig. 1. It is clearly seen how the data of the dedicated JLab/Hall C GEp-2 $\gamma$  experiment [13] improve on the precision of the pioneering GEp-I result [1,2]. Within their error bars of order 1 %, the JLab/Hall C experiment does not see any systematic  $2\gamma$ -effect on this observable. We effectively tried

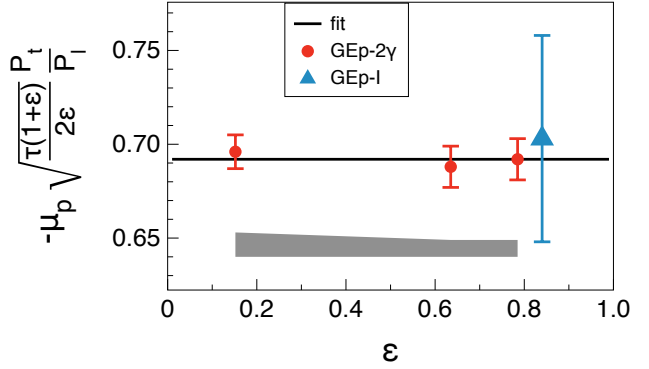


**Fig. 1.** The ratio  $-\mu_p \sqrt{\tau(1 + \varepsilon)/(2\varepsilon)} P_t/P_l$  as a function of  $\varepsilon$  for  $Q^2 = 2.5 \text{ GeV}^2$ . The data are from GEp-I (blue triangle) [1,2], and GEp-2 $\gamma$  (red circles) [13] : the error bars (grey band) show the statistical (systematic) errors respectively. The solid curve is an  $\varepsilon$ -independent fit, given by Eq. (9).

a fit of  $-\mu_p \sqrt{\tau(1 + \varepsilon)/(2\varepsilon)} P_t/P_l$  assuming an  $\varepsilon$ -independent part  $R$ , which in the  $1\gamma$ -limit equals  $\mu_p G_E/G_M$ , with  $\mu_p = 2.793$  the proton magnetic moment, supplemented with an  $\varepsilon$ -dependent part :

$$-\mu_p \sqrt{\frac{\tau(1 + \varepsilon)}{2\varepsilon}} P_t/P_l = R + B\varepsilon^c (1 - \varepsilon)^d. \quad (8)$$

Using a range of values for  $c$  and  $d$ , we found that the value  $B$  of is zero within the present error, and the extracted values of  $R$  are all equal within their error bars. Therefore we conclude that the precision of the present data [13] at  $Q^2 = 2.5 \text{ GeV}^2$  does not allow to extract an  $\varepsilon$ -dependent part, in addition to the constant value  $R$ . To extract the  $G_E/G_M$  ratio from the constant  $R$ , we are guided by the Regge limit assumption that the  $2\gamma$ -correction to  $P_t/P_l$  vanishes for  $\varepsilon \rightarrow 1$ . We therefore fit  $P_t/P_l$  by its  $1\gamma$ -value and obtain at  $Q^2 = 2.5 \text{ GeV}^2$  :

$$R = \mu_p G_E/G_M = 0.693 \pm 0.006_{\text{stat.}} \pm 0.010_{\text{syst.}} \quad (9)$$

To determine the  $\varepsilon$ -dependence of  $P_l$ , we conventionally divide by  $P_l^{\text{Born}}$ , which is calculated according to Eq. (4), using the value of Eq. (9) for  $G_E/G_M$ . Furthermore, the  $2\gamma$ -contribution to  $P_l$  is expected to be zero in both limits  $\varepsilon \rightarrow 0$  and  $\varepsilon \rightarrow 1$ . A perturbative QCD calculation (pQCD) [14,?] gives as limits :  $P_l/P_l^{\text{Born}} - 1 \rightarrow (1 - \varepsilon)^{1/2}$  for  $\varepsilon \rightarrow 1$ , and  $P_l/P_l^{\text{Born}} - 1 \rightarrow \varepsilon^2$  for  $\varepsilon \rightarrow 0$ . Although the data for  $P_l/P_l^{\text{Born}}$  do show a decrease for  $\varepsilon \rightarrow 0$ , in qualitative agreement with pQCD, the empirical fall-off at  $Q^2 = 2.5 \text{ GeV}^2$  is faster than the pQCD prediction. Therefore, we fit the data for  $P_l/P_l^{\text{Born}}$  using two different functional forms :

$$\begin{aligned} \text{Fit 1 : } P_l/P_l^{\text{Born}} &= 1 + a_l \varepsilon^4 (1 - \varepsilon)^{1/2}, \\ \text{Fit 2 : } P_l/P_l^{\text{Born}} &= 1 + a_l \varepsilon \ln(1 - \varepsilon) (1 - \varepsilon)^{1/2}. \quad (10) \end{aligned}$$

The fit to the data yields :  $a_l = 0.11 \pm 0.03_{\text{stat.}} \pm 0.06_{\text{syst.}}$  (Fit 1), and  $a_l = -0.032 \pm 0.008_{\text{stat.}} \pm 0.020_{\text{syst.}}$  (Fit 2).

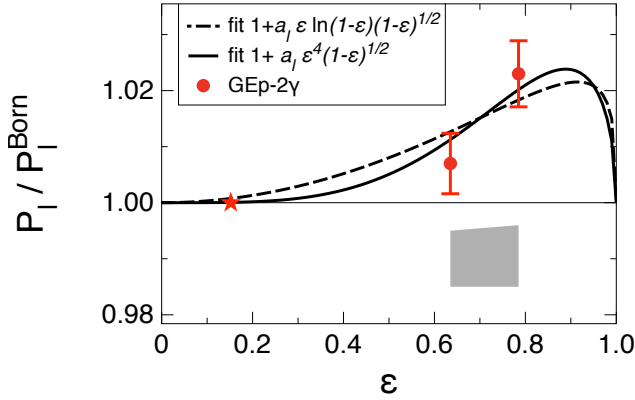


**Fig. 2.** The ratio  $P_t/P_l^{\text{Born}}$  as a function of  $\epsilon$  for  $Q^2 = 2.5 \text{ GeV}^2$ . The data points are from the GEp-2 $\gamma$  experiment (red circles) [13]: the error bars show the statistical errors, the grey band shows the systematic errors. The star indicates the  $\epsilon$ -value at which the data have been normalized to the value 1. The curves are two fits described in Eq. (10): Fit 1 (solid curve), Fit 2 (dashed curve).

We next fit the JLab/Hall A Rosenbluth measurements of  $\sigma_R$  [7], shown on Fig. 3 for  $Q^2 = 2.64 \text{ GeV}^2$ . The  $\sigma_R$  data show a linear behavior in  $\epsilon$ , suggesting the fit:

$$\sigma_R/(\mu_p G_D)^2 = a + b\epsilon, \quad (11)$$

where we follow the convention to factor out the dipole FF  $G_D \equiv 1/(1 + Q^2/0.71 \text{ GeV}^2)^2$ . The fit to the data in Fig. 3 yields:  $a = 1.106 \pm 0.006$  and  $b = 0.160 \pm 0.009$ .

To extract the three 2 $\gamma$ -amplitudes as well as  $G_E/G_M$  and  $G_M$  from the above three observables at a same  $Q^2$  value we have to make two assumptions. The first assumption was made in Eq. (8), where the  $\epsilon$ -independent term  $R$  fixes  $G_E/G_M$ , see Eq. (9). To fix the value of  $G_M^2$ , we make the assumption, that for  $\epsilon \rightarrow 1$  (Regge limit) the 2 $\gamma$ -correction to  $\sigma_R$  vanishes, i.e.  $\sigma_R(\epsilon = 1, Q^2) = G_M^2 + G_E^2/\tau$ . Using the  $G_E/G_M$  value extracted from the fit to  $P_t/P_l$ , and the fitted values of  $a$  and  $b$  entering Eq. (11), then allows to extract the value of  $G_M^2$  as:

$$\left(\frac{G_M}{\mu_p G_D}\right)^2 = \frac{a+b}{1 + (1/\tau)(G_E/G_M)^2}. \quad (12)$$

For  $Q^2 = 2.64 \text{ GeV}^2$ , our fit yields:

$$\left(\frac{G_M}{\mu_p G_D}\right)^2 = 1.168 \pm 0.010. \quad (13)$$

Having specified in Eqs. (3, 6, 7) the fits of the observables  $P_t/P_l$ ,  $P_l/P_l^{\text{Born}}$ , and  $\sigma_R$ , we next proceed to extract the 2 $\gamma$ -amplitudes  $Y_M$ ,  $Y_E$ , and  $Y_3$ . The data allow us to perform this analysis at a common value of  $Q^2 = 2.64 \text{ GeV}^2$ , where we neglect the small difference in  $P_t/P_l$  and  $P_l/P_l^{\text{Born}}$  between their values at  $Q^2 = 2.64 \text{ GeV}^2$  and their measured values at  $Q^2 = 2.5 \text{ GeV}^2$ . In Fig. 4, we

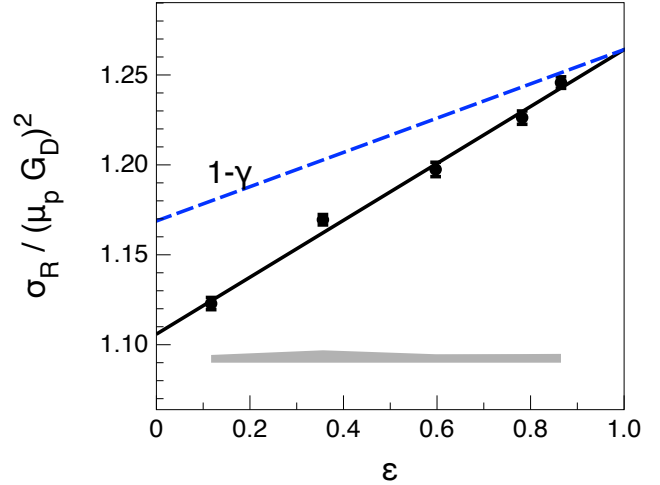


**Fig. 3.** Rosenbluth plots for elastic  $e^-p$  scattering:  $\sigma_R$  divided by  $\mu_p^2/(1 + Q^2/0.71)^4$  at  $Q^2 = 2.64 \text{ GeV}^2$ . Solid curve: linear fit to the JLab/Hall A cross section data (circles) [7]. Dashed curve: 1 $\gamma$ -result, using the slope from the polarization data for  $G_E/G_M$  [1,2,3]. The grey band shows the systematic errors.

show the result of this analysis for the 2 $\gamma$  amplitudes, together with their  $1\sigma$  error bands. One sees from Fig. 4 that the amplitude which is best constrained by the available data is  $Y_M$ . This is because the amplitude  $Y_M$  is mainly driven by the 2 $\gamma$ -effect in the cross section data, Eq. (3), which to good approximation is given by:  $\sigma_R^{2\gamma} \sim Y_M + \epsilon Y_3$ . One notices that the error bands on  $Y_M$  resulting from the two different fits of Eq. (10) for  $P_l$  largely overlap. Except in the large  $\epsilon$  region, the dominance of  $Y_M$  by the Rosenbluth data results in its approximate linear rise in  $\epsilon$ . For  $\epsilon \rightarrow 1$ ,  $Y_M$  has to become non-linear provided  $Y_M + \epsilon Y_3$  remains linear in the limit  $\epsilon \rightarrow 1$ , which we assumed in our present analysis. How far the linearity of the Rosenbluth plot extends when approaching  $\epsilon \rightarrow 1$  is of course an open question, which will be addressed by the results of a dedicated experiment [16]. In contrast to  $Y_M$ , the amplitudes  $Y_E$  and  $Y_3$  are mainly driven by the polarization data. One sees from Fig. 4 that the error bands overlap in the range ( $\epsilon > 0.6$ ) where data exist for all three observables. In the smaller  $\epsilon$  range, where there is no constraint from the polarization data, one sees clear deviations between the two different functional forms for the  $\epsilon$ -dependence. We checked that the same conclusion is reached for other forms. One further notices that in the region constrained by the polarization data, the amplitudes  $Y_E$  and  $Y_3$  are at the 2-3 % level and have opposite signs. This can be easily understood from Eq. (6) when neglecting the small terms in the 2 $\gamma$ -amplitudes which are multiplied by  $G_E/G_M$ . The leading 2 $\gamma$ -correction to  $P_t/P_l$  is to very good approximation proportional to  $Y_E + Y_3$ . The absence of 2 $\gamma$ -corrections in the data for  $P_t/P_l$  then implies  $Y_E$  and  $Y_3$  being of equal magnitude and of opposite sign. Furthermore, the value of  $Y_3$  is nearly entirely driven by the data for  $P_l$ . One indeed obtains from Eq. (7), when again neglecting the small  $G_E/G_M$  terms,

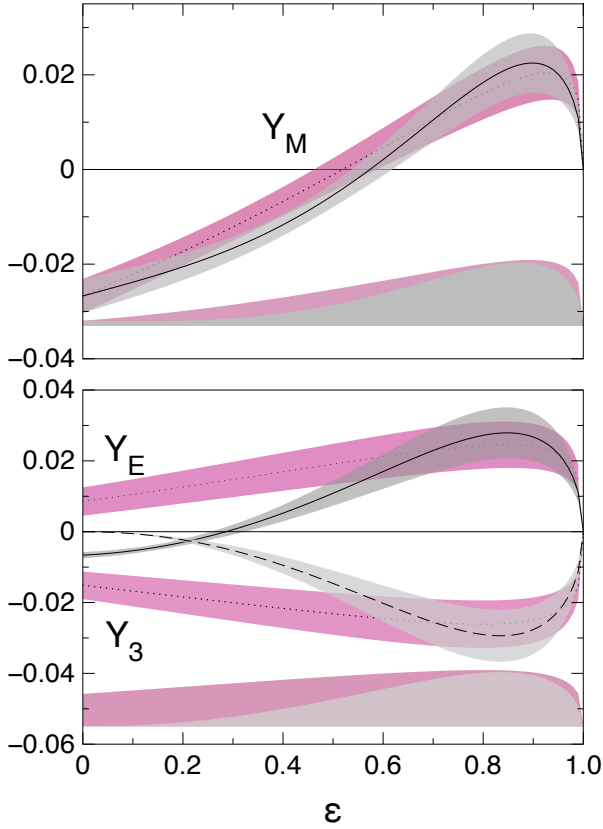


**Fig. 4.** The extracted  $2\gamma$ -amplitudes as a function of  $\varepsilon$  for  $Q^2 = 2.64 \text{ GeV}^2$  for the two fits of  $P_l$  in Eq. (10), with their  $1\sigma$  statistical error bands. Fit 1 : grey bands; Fit 2 : red bands. The horizontal bands at the bottom of the plots indicate the systematic errors.

$P_l^{2\gamma} \simeq -2\varepsilon^2/(1+\varepsilon) Y_3$ , therefore determining  $Y_3$ . To improve on the extraction of  $Y_E$  and  $Y_3$  will require a further improvement in precision of the polarization experiments.

We next discuss the ratio  $R_{e^+e^-}$  of  $e^+p/e^-p$  elastic scattering cross sections. The  $e^+p$  elastic scattering observables are obtained from the ones for  $e^-p$  by merely changing the sign in front of the  $2\gamma$ -amplitudes. A measurement of the ratio  $R_{e^+e^-}$  therefore provides a test of the  $2\gamma$ -amplitudes and is planned in the near future by several experiments [17,18,19]. In particular, the Olympus Collaboration at DESY plans to measure the  $e^+/e^-$  ratio for a value  $Q^2 \simeq 2.5 \text{ GeV}^2$  [19]. Our extraction of the  $2\gamma$ -amplitudes at  $Q^2 = 2.64 \text{ GeV}^2$  allows to predict the ratio  $R_{e^+e^-}$ , which is shown in Fig. 5, using Fit 1 in Eq. (10). We notice that for  $Q^2 = 2.64 \text{ GeV}^2$ ,  $R_{e^+e^-}$  rises linearly to small  $\varepsilon$ , reaching  $R_{e^+e^-} = 1.053 \pm 0.004$  for  $\varepsilon = 0.5$ . In Fig. 5, we also show results for the two other values of  $Q^2$  where the JLab high-precision Rosenbluth experiment [7] has taken data. At these higher values of  $Q^2$ , a systematic measurement of the  $\varepsilon$ -dependence of the polarization observables has not yet been performed. For our analysis of the  $Q^2 = 3.2 \text{ GeV}^2$  and  $Q^2 = 4.1 \text{ GeV}^2$

data, we therefore assumed that  $P_t/P_l$  can be fitted by its  $1\gamma$ -value proportional to  $G_E/G_M$  as extracted in [1,2,3]. We see from Fig. 5 that, for a fixed value of  $\varepsilon$ , the extracted ratio  $R_{e^+e^-}$  increases with  $Q^2$ .

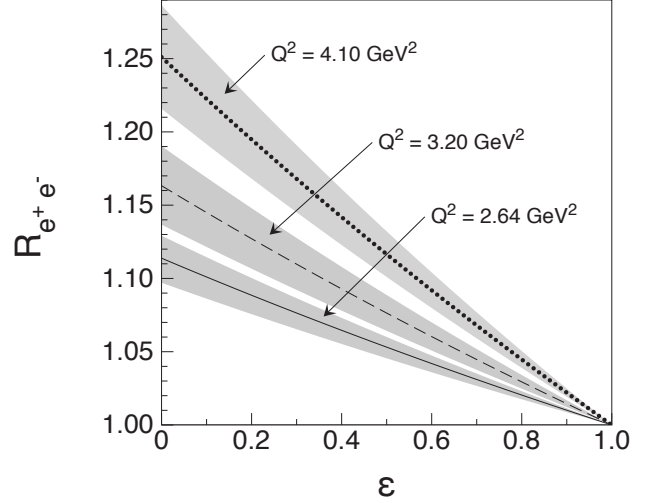


**Fig. 5.** Predictions for the  $e^+p/e^-p$  elastic cross section ratio  $R_{e^+e^-}$  as a function of  $\varepsilon$ , together with their  $1\sigma$  error bands.

Summarizing, in this work we provided a first combined analysis of high precision Rosenbluth data for elastic electron-proton scattering and recent measurements of the  $2\gamma$ -corrections to the polarization observables. As both experiments were performed at a similar  $Q^2$  value, we were able to perform an extraction of the three  $2\gamma$ -amplitudes at  $Q^2 = 2.64 \text{ GeV}^2$  using empirical results for three observables and assuming that for  $\varepsilon \rightarrow 1$  (Regge limit) the  $2\gamma$ -amplitudes vanish. We found that one amplitude ( $Y_M$ ) can be reliably extracted from the correction on the unpolarized cross section. The other two amplitudes are at the 2-3 % level and of opposite sign, partially cancelling each other in the polarization transfer ratio. Our extraction allowed us to provide a prediction of the  $e^+p/e^-p$  elastic cross section ratio, for which dedicated measurements by the Olympus@DESY experiment are underway. Over the measured range of this experiment, the  $2\gamma$ -corrections to the  $e^+p/e^-p$  elastic cross section ratio are predicted to vary in the 1 - 6 % range.

## Acknowledgments

The work of J.G. was supported by the Research Centre “Elementarkraefte und Mathematische Grundlagen” at the University Mainz. The authors like to thank J. Arrington, R. Milner, L. Pentchev, and C. Perdrisat for helpful communications and discussions.

## References

1. M. K. Jones *et al.* [Jefferson Lab Hall A Collaboration], Phys. Rev. Lett. **84**, 1398 (2000).
2. V. Punjabi *et al.*, Phys. Rev. C **71**, 055202 (2005) [Erratum-*ibid.* C **71**:069902 (2005)].
3. O. Gayou *et al.* [Jefferson Lab Hall A Collaboration], Phys. Rev. Lett. **88**, 092301 (2002).
4. A. Puckett *et al.*, Phys. Rev. Lett. **104**, 242301 (2010).
5. L. Andivahis *et al.*, Phys. Rev. D **50**, 5491 (1994).
6. M. E. Christy *et al.* [E94110 Collaboration], Phys. Rev. C **70**, 015206 (2004).
7. I. A. Qattan *et al.* Phys. Rev. Lett. **94**, 142301 (2005).
8. P. A. M. Guichon and M. Vanderhaeghen, Phys. Rev. Lett. **91**, 142303 (2003).
9. P. G. Blunden, W. Melnitchouk and J. A. Tjon, Phys. Rev. Lett. **91**, 142304 (2003).
10. Y.C. Chen, A. Afanasev, S.J. Brodsky, C.E. Carlson and M. Vanderhaeghen, Phys. Rev. Lett. **93**, 122301 (2004).
11. C. E. Carlson and M. Vanderhaeghen, Ann. Rev. Nucl. Part. Sci. **57**, 171 (2007).
12. J. Arrington, W. Melnitchouk and J. A. Tjon, Phys. Rev. C **76**, 035205 (2007).
13. M. Meiziane *et al.*, arXiv:1012.0339 [nucl-ex].
14. D. Borisyuk and A. Kobushkin, Phys. Rev. D **79**, 034001 (2009).
15. N. Kivel and M. Vanderhaeghen, Phys. Rev. Lett. **103**, 092004 (2009).
16. JLab experiment E-05-017, spokesperson J. Arrington.
17. J. Arrington *et al.*, arXiv:nucl-ex/0408020.
18. JLab/CLAS experiment E-07-005.
19. Proposal at DESY [Olympus Collaboration], (2008).